

## SEISMIC VULNERABILITY ASSESSMENT OF A 17<sup>TH</sup> CENTURY COLONIAL ADOBE CHURCH IN THE CENTRAL VALLEY OF CHILE

N. C. PALAZZI<sup>1,2\*</sup>, G. MISSERI<sup>3</sup>, L. ROVERO<sup>3</sup> AND J.C. DE LA LLERA<sup>1,2</sup>

<sup>1</sup>Research Center for Integrated Disaster Risk Management (CIGIDEN),

<sup>2</sup>Pontificia Universidad Católica de Chile

Avda. Vicuña Mackenna 4860, Macul, Santiago, Chile

e-mail: nuriachiara.palazzi@cigiden.cl (\*corresponding author), jcllera@puc.ch

<sup>3</sup>Department of Architecture, University of Florence

Piazza Brunelleschi, 6, 50121, Firenze, Italy

e-mail: giulia.misseri@unifi.it, luisa.roveo@unifi.it

**Keywords:** Historical Structure, Unreinforced Adobe Masonry, Seismic Vulnerability

**Abstract.** *This paper focuses on the seismic vulnerability assessment of the San Judas Tadeo's church in Malloa (Chile), an iconic example of Colonial Chilean architecture. This small adobe structure is a single-nave building consisting of the main nave, a bell-tower located in the façade, two external wooden galleries and additional units such as the sacristy, chapel, and two services areas.*

*The Church has survived several strong earthquakes larger than  $M_w > 8$ . Besides, after the February 27<sup>th</sup>, 2010 Maule event it showed remarkable resilience due to the implementation of traditional timber retrofits inserted in the earthen walls. The use of traditional wooden devices such as bond beams, corner keys, and wooden gables, proved to be effective solutions against strong earthquakes.*

*Therefore, this church appears as a relevant case of the use of seismic resistant constructive techniques of the 17<sup>th</sup> century colonial architecture and the study of its seismic behaviour holds great interest and relevance.*

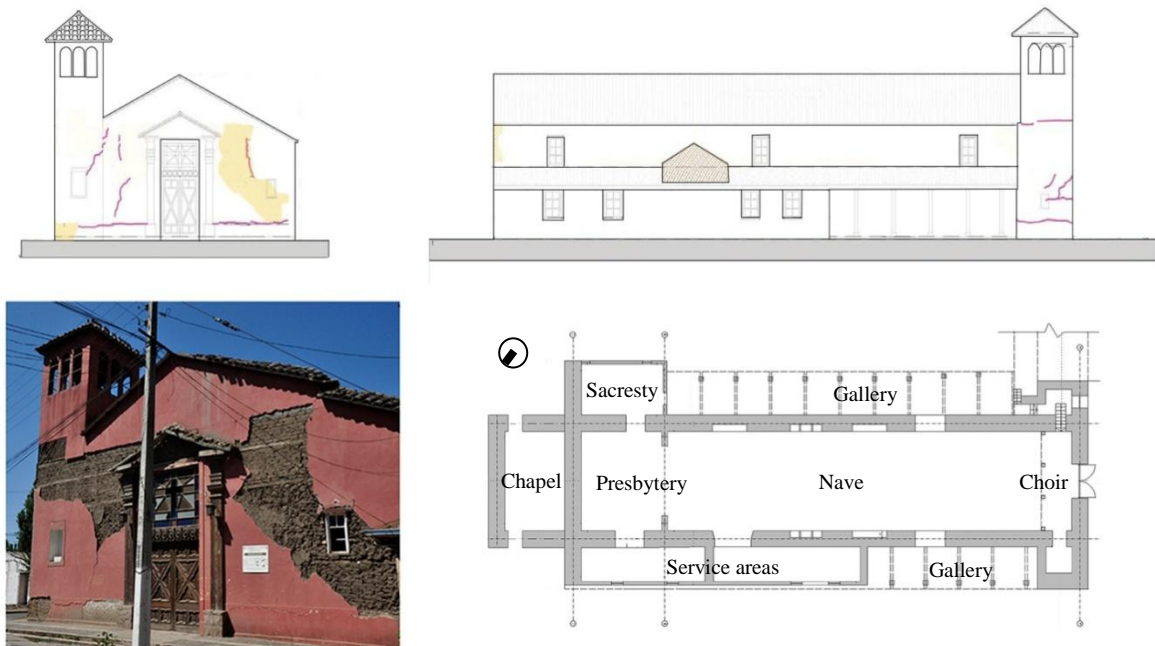
*Aimed to assess the seismic performance of the monument, a complete preliminary study of the church was carried out using a multi-level approach comprising historical research, in situ surveys, crack pattern analysis, physical and mechanical characterization of materials, and structural analyses. In particular as part of an ongoing research, linear and incremental kinematic approaches of limit analyses have been employed with the aim of interpreting the local mechanisms activated during the 2010 Maule earthquake. In these models, the effect of friction on masonry-to-masonry and timber-to-masonry interfaces was considered with promising outcomes.*

*This study results prove the general validity in the field of timber seismic retrofitting of unreinforced adobe buildings.*

## 1 INTRODUCTION

San Judas Tadeo is the parish of the community of Malloa (-34.442247, -70.943377), a rural village of 12,000 inhabitants located in Cachapoal Province, Libertador General Bernardo O'Higgins region (VI), at 113 km south of Santiago.

The first parish was erected in 1635 and was completely destroyed by the May 13, 1647 (Ms~8) Santiago earthquake [1]. The current parish was founded in 1845 under the avocation of San Juan Batista, but years later the devotion to San Judas Tadeo prompted a name change. The fervor of the community for this saint, known as the employer of the difficult causes, arose in 1887 during an epidemic of cholera. The tragedy touched the citizenry and settled in the collective memory of the village. Thus, the San Judas Tadeo church became a significant religious and civil Landmark of Malloa. It was declared Historic Conservation Zone (ZCH) according to Art. 60 of the General Urban Planning and Buildings Law; and it is now acknowledged as Historical Monument according to Law N°17.288 of National Monuments [2]. This parish was constructed following the typical architectural, constructive and structural features of Colonial style of the Chilean central valley [3, 4]. The morphology of the structure consists of an austere rectangular plane of a single-nave, and additional units built later. The plane is 45.1m long in the longitudinal direction, 9.9m wide in the transversal direction, with a maximum roof height of 9.92m, accommodating 500 people.



**Figure 1:** View of the façade of the church and current plan, façade and lateral view[5]

The church has an area of 815.84 m<sup>2</sup>, and it features a central rectangular space oriented north-east south-west, a sacristy adjacent to the western wall, and two additional service areas located respectively on the northern and eastern walls. The main nave is divided in three sectors (choir, nave and presbytery, Fig. 1), and has undergone several modifications over the time thus different construction techniques and materials are distinguishable.

## 2 CONSTRUCTION PHASES AND MAIN INTERVENTIONS

Malloa village is located in the territory of an indigenous village which motivated the installation of Franciscan convent which back to 1635 and was dedicated to San Antonio, one of the oldest in the VI region. The first temple was completely destroyed by the 1647 earthquake and a new Parish was erected in 1662, under the invocation of San Antonio de Papua. The first records date back to 1824. The current building was founded on the 17<sup>th</sup> November 1845, although there is no documentation indicating which parts of the 1662 temple were reused. After the 1928 Talca earthquake (7.6Mw), the complex suffered from considerable damage, and in the same year it was restored [1]. Despite the lack of historical information about the parish, during direct surveying activities carried out by the authors, it was possible to recognize the original structure and the main subsequent construction phases. In fact, through the detection of construction techniques corresponding to specific historical periods and the survey of structural discontinuities, three main construction phases have been identified.

The first period corresponds to the original block composed by the main nave (choir loft, nave and presbytery) and the base of the bell tower at the side of the facade (dated back 1662-1824).

The second construction phase corresponds to the parish enlargement with northern and eastern service areas attached to the main block. These areas were built with *adobillo*, a system originated in the Valparaiso region in the middle of 19<sup>th</sup> century [6].

Finally, during the third construction phase (undated) a chapel and a sacristy were erected with adobe masonry walls, simply juxtaposed to the rear and west walls, respectively. The actual configuration of the Parish is the result of seismic consolidation interventions and reconstructions during the past centuries characterized by different building techniques and materials, which present different structural behaviors. Probably after the 1985 Valparaiso earthquake (Mw8.0), the parish suffered considerable damage in the façade and bell tower, which were then reconstructed by wooden walls and reinforced through timber ring beams in the upper part. After the 2010 Maule earthquake (Mw 8.8), the church incurred in significant damages due to severe crack pattern that induced separation among walls. Structural damage amplified due to rising damp and local deformation. In 2016, Arias Arquitectos carried out a wide conservation project that addressed the whole parish [1].

## 3 ARCHITECTURAL ELEMENTS AND PROPERTIES OF MATERIALS

The parish has undergone several modifications over the time. Consequently, different construction techniques and materials are observable. According to the historical analysis, three traditional constructive systems for masonry walls were recognizable: (i) 4-wythe English bond with the insertion of timber elements, named W01; (ii) *adobillo*, which is a mixed wooden-earth technique where a thin timber frame interlocks a single-wythe shiner bond, named W02; and (iii) stacked 2-wythe masonry with header bond, labelled W03. The central nave walls (W01) are adobe masonry with the insertion of timber elements within the thickness, which are traditional seismic resistant technique of the local colonial culture. These timber reinforcements are composed of horizontal and transversal elements.

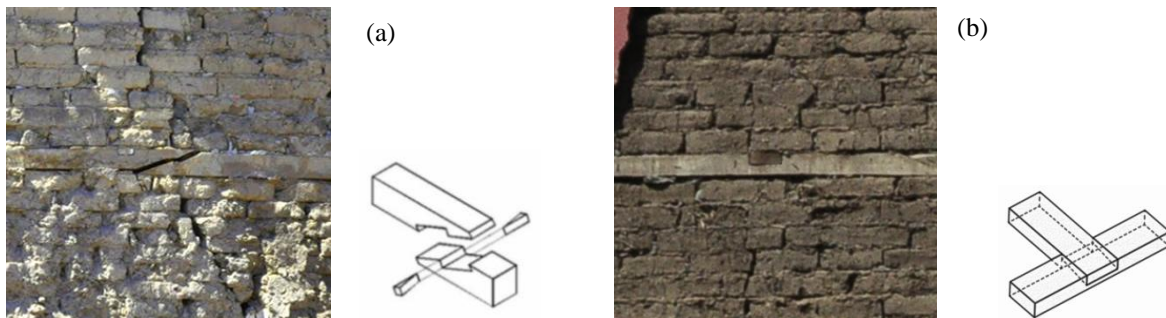
The wooden horizontal-elements run along the walls of the central nave and the base of bell tower, and transversal-elements across the full whole thickness. The horizontal elements have

a section of 10x20cm located about every 1.8-2.7m, while the wooden transversal ones are about 5x10cm every 2.25m. This traditional construction practice exploits the mechanical proprieties of wood, improving the out-of-plane bending capacity and in-plane shear resistance of adobe walls. The woodworking joints constitute the main seismic weakness of this system when subjected to the seismic motion. In San Tadeo parish there are two types of joints: *hooked scarf* and *halved joints*.

The *hooked scarf joint*, which is employed to connect the wooden horizontal elements, is a traditional method of joining two members end-to-end. This technique offers remarkable capacity in the longitudinal direction because it extends resistive area of the joint, thus maximum allowed force heightens, but the link mostly depends on the mechanical fastener employed to keep the joint closed, Fig. 2a.

The *halved joint*, another traditional link, is used to join two orthogonal members by removing material from each at the point of insertion so that they overlap, Fig. 2b. The amount of material removed is equal to half of the width, so the connections are weak and prone to split.

Following the 2010 Maule earthquake, the failure of the joint interlocking between wooden elements is observed in particular for the hooked scarf joint. The link failures are shown by the slippage between the wooden elements in the horizontal direction, determining the propagation of vertical and diagonal cracks along the entire height of the wall, see Fig.2a.



**Figure 2:** Traditional timber joints in Malloa parish: (a) hooked scarf joint, and (b) halved joint

The W01 walls of the central nave (thickness 1.45m) are made of 4-wythe earthen wall, of adobe brick with dimensions 35x60x15cm, bond by an earth mortar. The connections among orthogonal walls of the central nave, despite the absence of bond, consist of using wooden *corner keys* and *bond beams*. These traditional strengthening solutions induce walls working together even when the bonds between perpendicular walls crack during an earthquake [7], as it has been observed after 2010 Maule earthquake in the rear wall of central nave of Malloa church.

The slender walls of two service areas located on lateral northern wall of central nave are made of *adobillo*, another traditional mixed wood-earth single-leaf wall (W02). The *adobillo* wall of Malloa parish is the result of traditional local anti-seismic techniques and modern materials introduced in 19<sup>th</sup> century. It is composed by vertical wooden logs (10x10cm) every 75cm, horizontal wooden twigs (10x30cm), adobe blocks (60x30x10cm) of shiner course, and interior and exterior earth plaster with diagonal steel wires. This constructive system, originated in Valparaiso, generally, uses a particularly shaped earth

blocks having two 1'x1' notches in the headers of block that allow to fix the *adobillo* to wooden logs [6]. However, these efficient links between earthen blocks and wooden elements are absent in the *adobillo* walls of San Tadeo Parish.

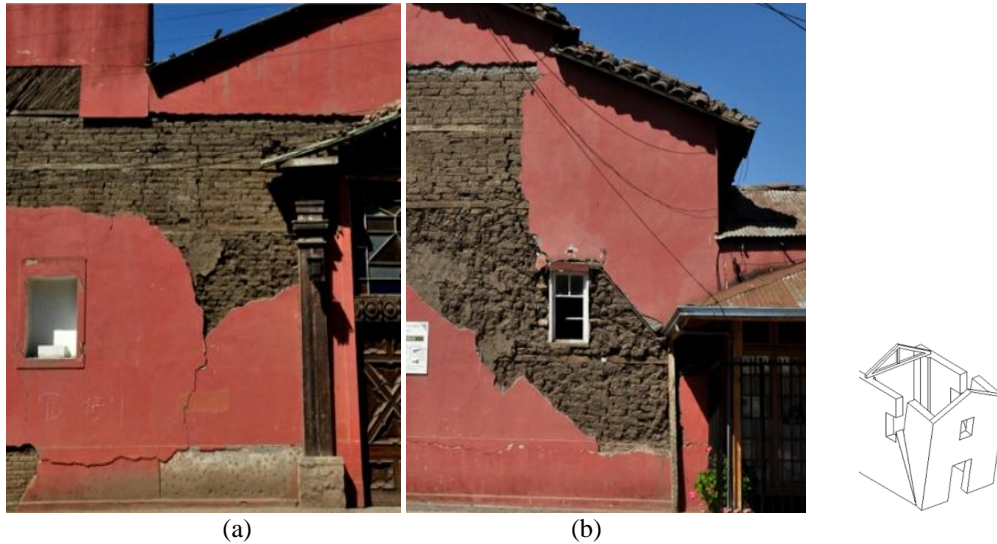
Finally, the masonries of chapel and sacristy, adjacent to the presbytery walls, were built with adobe masonry W03, block dimensions of 35x70x15cm. The W03 is double-leaf masonry without blocks crossing the whole thickness which can generate a transversal locking, the *diatones*. Consequently, the wall is composed into sections simply positioned one next to the other, very vulnerable to the out-of-plane seismic actions. Furthermore, this adobe masonry is characterized by a head bond resulting in lower shear strength than a monolithic panel and an inadequate seismic behavior[8].

In order to define the mechanical proprieties of adobe blocks, the values suggested by Chilean Standard [9] for adobe structures have been used. The Young's modulus  $E=200$  MPa, compressive strength  $f'_m=0.6$  MPa, and shear strength  $v'=0.025$  MPa of adobe masonry are assumed. The wooden trusses of the roof structures consist of oak elements (*Nothofagus oblique*), with density ( $\gamma=624\text{kg/m}^3$ ), compressive strength ( $f_{m,medium}=46.65\text{MPa}$ ), and shear strength ( $v'_{0,medium}=6.08\text{MPa}$ ). Finally, to the aim of characterizing the soil mechanics and the foundation type, four excavations located near the west wall of the north chapel [E1], the south area of parish house [E2], the north area of parish house [E3], and the inner courtyard [E4], with a depth of 3m, 2.6m, 3m, and 3m respectively were carried out by [10]. Based on the Chilean Code NCH433of 96 [11] and D.S.61, 2011[12]the soil, having medium dense soil,  $V_{s30} = 332 \text{ ms}^{-1}$ , and shear strength non-drained minor of 0.05MPa, was classified as soil type D, with soil coefficient  $S=1$ .

### 3 ASSESSMENT OF CRACK PATTERN

The San Juan Tadeo parish has suffered severe damage after the 2010 Maule earthquake. In particular, different seismic behaviors depending on the construction techniques were observed in the main block (W01), the service areas (W02), and the sacristy and rear chapel (W03). The main block of Malloa parish consists of heavy and thick walls (slenderness  $H/t=6.8$ , where  $H$  and  $t$  are the height and thickness of wall respectively), wooden beam bonds within the thickness and corner keys. Despite this, the traditional anti-seismic system, based on the use of timber, keeps the walls working together (*box-behavior*). In the main façade, the failure of joints, which used to attach (kink) end-to-end two horizontal members, aided the propagation of deep vertical cracks. The compound overturning of the thick façade ( $H/t=5.2$ ) is highlighted by vertical cracks passing through the wall thickness (Fig.3a-b) and the disconnections between the façade and the longitudinal side walls, internally observable. Furthermore, the presence of timber corner keys provides reinforcement improving the post-elastic behavior of the walls. Thus, a part of the longitudinal side walls and the façade continue to work together. The diagonal cracks observed in the longitudinal walls highlight the activation of an overturning mechanism that involved the façade and triangular portions (two side wings) of the longitudinal walls around a horizontal hinge, located at 72cm above the ground level. The shape of façade macro-element depends on several factors, mainly: the length and number of corner keys, the masonry-wood friction, and the distance between openings and wall-corner. Significant vertical cracks are also visible in the upper part of longitudinal side walls of the nave, mainly near the openings of windows

and doors. This crack pattern, observable in the internal (Fig. 4a) and external (Fig. 4b) elevations of side walls, suggests the activation of out-of-plane failure mechanisms, triggered by horizontal flexure of the wall, and involving the upper part of the discretized longitudinal walls between the openings (Fig. 4). The rotation towards the outside occurs around a horizontal hinge defined by the crack in correspondence of the wooden horizontal reinforcements of the W01, located at 4.6m above ground level.



**Figure 3:** Deep vertical cracks in the main façade[5]

Diagonal shear cracks caused by the seismic action along the in-plane direction of the wall nave were observed near the openings, in correspondence with the spandrels.



**Figure 4:** Deep cracks observable in the (a) internal and (b) external elevations of side walls [5]

The influence of the carpentry links (Fig.2a) on the global seismic behavior of the structure is often neglected. Nevertheless, as demonstrated by the activation of the local failures in the façade and side walls of the parish, it is essential to analyze these particular behaviors in order

to reach a complete understanding. Concerning the presbytery wall, the level of connections obtained through the corner keys at different heights is sufficient to generate restraint with the longitudinal walls. Nevertheless, localized vertical crushing in the corner occurs due to the absence of masonry bonds. The fracture lines are in correspondence of longitudinal wall planes. With respect to the chapel, several local collapses involving the external leaf of the two-leaf adobe masonry (W03) were observed. Two double-leaf-wall overturning mechanisms triggered, determining the collapse of the external leaf, with trapezoidal shape in the upper part of the wall. The low quality of W03 masonry, the absence of good bond, and the presence of big openings close to the wall corner affected the shape of the macro-element. Furthermore, the collapse of the corner of sacristy was observed. The timber consolidation interventions of bell-tower cell and façade gable avoided local collapses and significant damage, guaranteeing ductility and allowing oscillation without loss of equilibrium. These traditional strengthening techniques showed high efficacy in avoiding complete loss and collapses after the several earthquakes that have hit the church.

#### 4 STRUCTURAL ANALYSIS THROUGH LOCAL MECHANISMS

The results described in previous Sections (2 and 3) suggest that preliminary structural analyses should be focused on the recurring failure mechanisms of the observed macro-elements, which have exhibited significant damage during the past earthquakes. With the aim of assessing the vulnerability levels of identified macro-elements, considering the out-of-plane behavior, linear kinematic analyses (LKA) were conducted according to Chilean Codes [9], [11] and [12] combined with the provision of the Italian Code NTC2008 [13], and the Guidelines of Cultural Heritage [14]. Firstly, the layout of the mechanisms that are most likely to be activated in the Parish has been defined for the current state. The results of LKA (Kinematic multiplier  $\lambda_0$ , Participating Mass  $M^*$ , Mechanism Activation Acceleration  $a_0^*$ , the Demand Acceleration at ground and elevated levels) are shown in Table 1.

The Parish damage can be interpreted as the activation of the out-of-plane collapse mechanisms that involved: (i) the main façade; (ii) the side walls of main nave, and (iii) the walls of the sacristy and chapel.

- (i) Concerning the main building, all detected out-of-plane mechanisms are simple overturning of rigid sub-blocks that activated on the west and east lateral walls around a cylinder hinge placed 4.6m off the ground level considering the basic treatment of limited compressive strength, LWe1, LWe2, LWe3, LWe4, LWe5, and LWw1, LWw2, LWw3, LWw4, LWw5. All mechanisms are shown in Table 1.
- (ii) Only in the case of the sacristy walls the triggered mechanisms involved the external leaf of masonry, which collapsed; these mechanisms are labelled LWw5, LWe6 and LWe7. The overturning of the external leaf of a masonry is one of the weakest mechanisms since the stabilizing action of the weight can be reduced up to 4 times if compared to a monolithic block.
- (iii) Finally, different mechanism types for the out-of-plane behavior of main façade, FA, have been considered. In particular, compound overturning with basic treatment of limited compressive strength (CO-FA), simple overturning with sliding of timber elements hindered by masonry-to-timber frictional forces (SO-FA) and the compound overturning with cohesionless Coulomb failure criteria (COC-FA) have been analyzed.




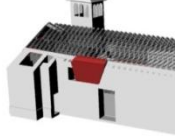
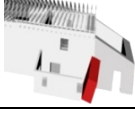


#### 4.1 Out-of-plane failure assessment through standard limit analysis

After the identification of the layout of the failure modes and the forces involved in the mechanisms, the kinematic multiplier of the horizontal equivalent forces producing the activation of the mechanisms,  $\lambda$ , has been determined and shown in Table 1. Consequently, the  $\lambda$  has been converted into acceleration capacity  $a_0^*$ , according to codified procedures [14] and [15] based on the hypotheses of absence of tensile strength of masonry; absence of sliding between the interconnected rigid blocks; and limited compressive strength of masonry.

$$\lambda(\sum_{i=1}^n P_i \cdot \delta_{xi}) = \sum_{i=1}^n P_i \cdot \delta_{yi} \cdot \delta_{yi}; \quad a_0^* = \frac{\lambda \sum_{i=1}^{n+m} P_i}{M^*}; \quad M^* = \frac{(\sum_{i=1}^n P_i \cdot \delta_{xi})^2}{g \cdot (\sum_{i=1}^n P_i \cdot \delta_{xi}^2)} \quad (1)$$

where:  $\lambda$  is the kinematic multiplier;  $P_i$  is the  $i$ -th load;  $\delta_{xi}$  is the virtual horizontal displacement of the gravity center of the  $i$ -th load  $P_i$ ;  $\delta_{yi}$  is the virtual vertical displacement of the gravity centers of the  $i$ -th load  $P_i$ ;  $M^*$  is the participating mass; and  $a_0^*$  is the acceleration capacity;

**Table 1:** Results of Linear Kinematic Analysis of current state: Kinematic multiplier  $\lambda$ , Participating Mass  $M^*$ , Mechanism Activation Acceleration  $a_0^*$ , equ. (2) for the Demand Acceleration ( $DA$ ) at ground level  $D_{ag}$  equ. (3) for the Demand Acceleration at an elevated level,  $D_{al}$ ; and safety index  $Is_{IKA}$  evaluated as  $a_0^*/DA$ .

<i>ID</i>	<i>State Current</i>	$M^*$ [kN]	$\lambda_i$	$a_0^*$ [m/s <sup>2</sup> ]	<i>DA</i> [m/s <sup>2</sup> ]	$Is_{IKA}$ [-]
Fa-CO		2286	$\lambda=0.263$	1.92	$D_{ag}=5.3$	0.362
LW1w		328	$\lambda=0.397$	3.46	$D_{ag}=5.3$	0.65
LW2w		239	$\lambda=0.212$	1.99	$D_{al}=4.1$	0.38
LW3w		201	$\lambda=0.362$	4.87		0.92
LW4w		212	$\lambda=0.445$	4.25		0.80
LW5w		134	$\lambda=0.183$	1.34	$D_{ag}=5.3$ $D_{al}=3.1$	0.25
LW1e		235	$\lambda=0.378$	3.25	$D_{ag}=5.3$	0.61
LW2e		312	$\lambda=0.411$	3.7	$D_{al}=4.1$	0.7
LW3e		262	$\lambda=0.384$	3.39		0.64
LW4e		268	$\lambda=0.367$	4.01		0.75
LW5e		397	$\lambda=0.334$	2.92	$D_{ag}=5.3$	0.55
LW6e		95.6	$\lambda=0.099$	0.722	$D_{ag}=5.3$ $D_{al}=3.2$	0.14
LW7e		47.4	$\lambda=0.242$	1.756	$D_{ag}=5.3$	0.33



For a more realistic simulation in computing the kinematic multiplier  $\lambda$ , the limited state due to masonry crushing for compressive stress ( $f_m=1.2\text{MPa}$ ) has been considered assuming the inward displacement of the cylinder hinge,  $t = 0.05\sum_{i=1}^n W_i (f_d l)^{-1}$ , which depends on  $i$ -th self-weight,  $W_i$ , the width of the wall,  $l$ , and the design compressive strength,  $f_d=f_m(\gamma_M)^{-1}$ .

The safety conditions require that the structural capacity ( $\alpha_0^*$ , equ.1) must be equal or greater than the seismic demand  $D_{ag}$  [ $\text{m/s}^2$ ], calculated according to the NCh433 Chilean Code (for soil type D). When the masonry macro-element is placed at the ground level it imposes:

$$\alpha_0^* \geq a_g(P_{VR})Sq^{-1}=5.3 \text{ ms}^{-2} \quad (2)$$

Thus,  $D_{ag}$  depends on  $a_g(P_{VR})$ , the peak ground acceleration with an exceeding probability of 10% in 50 years;  $S$ , the sub-soil factor (here assumed equal to 1); and  $q$ , the behavior factor to account for energy dissipation capacity of the unreinforced masonry structure, equal to 1.5 according to [15]. In the case of the macro-elements placed higher than ground level, a further check must impose the input demand amplified by the effect of height  $D_{al}$  [ $\text{m/s}^2$ ]:

$$\alpha_0^* \geq S_e(T_1)\Psi(Z)\gamma \quad (3)$$

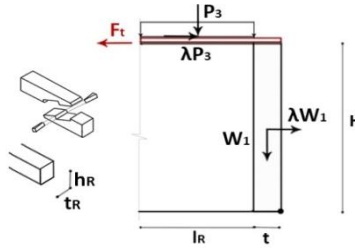
It is in dependence on the design spectrum acceleration,  $S_e(T_1)$ , with respect to the first vibration period of the macro-block  $T_1$ , being  $T_1=0.09 H^{3/4}$  (characterizing the adobe buildings, [16]). Finally  $\psi(z)=Z/H$  is a function depending on the height from the foundation of the centroid of the weight forces applied on the rigid bodies,  $Z$ , on the total height of the building from the foundation,  $H$ , and on  $\gamma=3N/(2N+1)$ , which corresponds to a modal participation coefficient, depending on  $N$  number of floors.

## 4.2 Out-of-plane failure assessment through non-standard limit analysis

### 4.2.1 Simple overturning of main façade considering sliding at timber-masonry interface

Kinematic multiplier for the simple overturning of façade has been also calculated considering that restraining forces at timber-masonry interface due to frictional mechanisms can arise, in case the uppermost ring beam is not well anchored to the masonry. The resistive friction force,  $F_t = 2 \mu p t_R l_R$  depends on the dimensions of the restraining device (Table 2), as proposed in [17]. In the expression of  $F_t$ ,  $\mu_t$  is the friction coefficient between timber and earth masonry;  $p$  is the force per unit surface of the slab;  $t_R$  is the thickness of the longitudinal timber element,  $l_R$  is the unit-length of the reinforcement (*ring beam*).

**Table 2:** Simple overturning of main façade (SO-FA) considering sliding at timber-masonry interface



ID	$M^*$ [kN]	$\lambda_t$	$\alpha_0^*$ [ $\text{m/s}^2$ ]	DA [ $\text{m/s}^2$ ]	$I_{sIKA}$ [-]
SO-FA	1691	0.167 ( $\mu=0.3$ )	1.63	$D_{ag}=5.3$	0.308
		0.168 ( $\mu=0.5$ )	1.64		0.31
		0.169 ( $\mu=0.6$ )	1.65		0.311

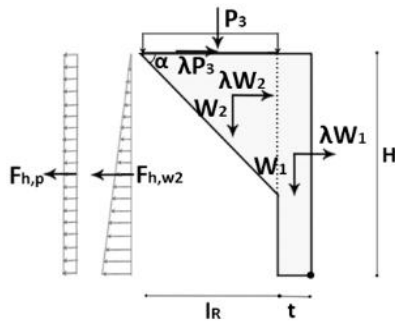
According to [18] different values of the wooden-masonry friction coefficient have been considered,  $\mu=0.3$ , 0.5 and 0.6, as shown in Table 2. It is relevant to note that the

contribution of the ring-beam is significant when a good anchoring of timber joints exists, i.e. when the timber end-to-end joints are working well since  $l_R$  significantly increases and consequently also  $\lambda_t$ . The values obtained for  $\lambda_t$  constitute an upper (unsafe) threshold to the corresponding value of  $\lambda$ .

#### 4.2.2 Compound overturning of main façade considering the cohesionless Coulomb's failure criterion

The crack pattern of the Malloa façade, in which diagonal cracks (inclination of the crack slope to the vertical equal to  $\beta = 1.052\text{rad} \sim 60.25^\circ$ ) are visible on the orthogonal walls, denotes a good interlocking among them. The contribution of the timber reinforcement is considered and slope to the horizontal that fracture forms is identified through the minimum angle  $\alpha$ . The contribution of friction in the analysis of façade compound overturning is considered according to [17, 19, and 20] through limit analysis applied to non-standard materials. An added system of forces [17, 19, and 20] acting in the direction opposed to that of the earthquake action, and proportional to self-weights and overburden loads through the friction coefficient has been modelled:  $F_{h,w2}$ , the horizontal force offered by dry friction and due to self-weight, which depends on the compression found at each block interface and equal to  $F_{h,w2} = \{[H(H \tan \theta + t)]/2\} \gamma b \mu$ ; and  $F_{h,p}$ , the contribution offered by dry friction due to overburden loads, and equal to  $F_{h,p} = p H \tan \theta b \mu$ , where  $\gamma$  is the specific weight of masonry;  $\mu$  is the friction coefficient related to masonry;  $H$  is the height of the façade macro-element;  $b$  is the thickness of the considered wall;  $\theta = v/t$  is the staggering ratio angle with  $v$  overlapping length among two blocks and  $t$  block thickness; and  $p$  is the force per unit surface of the slab (Table 3).

**Table 3:** Compound overturning of main façade (COC-FA) considering the cohesionless Coulomb's failure criterion with frictional capacity expressed at all bed joints identifying the crack.



ID	$M^*$ [kN]	$\lambda_{t-\mu}$	$\alpha_0^*$ [m/s <sup>2</sup> ]	DA [m/s <sup>2</sup> ]	$I_{S_{IKA}}$ [-]
COC -FA	2141.8	0.809( $\mu=0.2$ )	6.4	$D_{a0}=5.3$	1.19
		0.949( $\mu=0.3$ )	7.4		1.4
		1.032( $\mu=0.4$ )	8.1		1.52

The inclinations of crack slopes to the horizontal, characterising mechanism layouts and identified through complementary angles of  $\alpha$ . For  $\mu = 0.2, 0.3$  and  $0.4$ , the complementary angles of  $\alpha$  obtained minimizing  $\lambda_{t-\mu}$  are respectively  $1.176\text{rad} (\cong 67^\circ)$ ,  $0.833\text{rad} (\cong 48^\circ)$  and  $0.670\text{rad} (\cong 38^\circ)$ . Considering the case of lower friction coeff ( $\mu = 0.2$ ), which already leads to non-conservative values, it can be observed that the mechanism layout is remarkably close to the staggering mechanism ( $\theta = 1.165\text{rad} \cong 67^\circ$ ), showing that the contribution of friction might be less relevant. This consideration supports the hypothesis that the resistive forces necessary to understand the actual mechanism are cohesive forces as investigated in [17].

## 5. CONCLUSIONS

In this paper a preliminary analysis of the seismic performance of a timber-reinforced colonial church that survived strong earthquakes, the Malloa parish, has been assessed. All OOP failures, detected during survey activities following the 2010 Maule earthquake, were assessed through standard limit analysis (LKA) considering the basic treatment of limited compressive strength. Results of LKA for OOP failure of compound façade offered an unsatisfactory safety assessment, safety index  $I_{S_{IKA}}=0.362$ . Regarding the OOP simple overturning of west and east lateral walls of central nave offered safety indexes between  $0.33 \leq I_{S_{IKA}} \leq 0.92$ . While, for the overturning mechanisms of external leaf of masonry walls (LW5w and LW6e), the safety indexes are between  $0.14 \leq I_{S_{IKA}} \leq 0.25$ . In this case the collapse has already occurred during 2010 Maule earthquake.

For a more realistic simulation in computing of the kinematic multiplier,  $\lambda$ , non-standard limit analyses have been also carried out. Simple overturning of main façade has been also calculated considering that restraining forces at timber-masonry interface due to frictional mechanisms can arise, in case the uppermost ring beam is not well anchored to the masonry. The results show that the contribution of the ring-beam is significant when a good anchoring of timber joints exists, i.e. when the timber end-to-end joints are working well since  $l_R$  significantly increases and consequently also  $\lambda_r$ . The values obtained for  $\lambda_r$  constitute and upper (unsafe) threshold to the corresponding value of  $\lambda$ .

Moreover, contribution of friction in the analysis of façade compound overturning is considered through limit analysis applied to non-standard materials, take into account: the horizontal force offered by dry friction and proportional to self-weights and overburden loads. Although offering reasonable mechanism layout (i.e. surveyed) values of the load multiplier provide a non-conservative estimation of the vulnerability.

Local-level analysis have provided a reliable assessment of the OOP mechanisms of main façade, lateral walls and chapels. Results suggest that vulnerability could have been successfully reduced through punctual interventions that make use of traditional retrofitting technologies based on the use of wood, instead of extensive and invasive solutions somehow partially incompatible

**Acknowledgements.** This work was supported by the Research Center for Integrated Disaster Risk Management (CIGIDEN), CONICYT/FONDAP/15110017, and by the SIBER-RISK Regular Fondecyt project CONICYT/FONDECYT/1170836.

## REFERENCES

- [1] Arias Arquitectos, and Fercovic, G. 2011. Ficha técnica de daño y oferta de servicios. Informe de la Evaluación Preliminar de Daños Provocados por el sismo de 2010, Chile: Ilustre municipalidad de Malloa, Departamento de Proyecto.
- [2] Consejo de Monumentos Nacionales, (CMN) Ministerio de 900 Educación. 2011. Chilean law of monuments 17.288. Accessed March 23, 2017. <http://monumentos.cl>
- [3] Palazzi, N. C., Rovero, L., De La Llera, J. C., Sandoval, C. (2019). Preliminary Assessment on Seismic Vulnerability of Masonry Churches in Central Chile. *International Journal of Architectural Heritage*, 1-20

- [4] Palazzi, N. C., Favier, P., Rovero, L., Sandoval, C., & de la Llera, J. C. (2020). Seismic damage and fragility assessment of ancient masonry churches located in central Chile. *Bulletin of Earthquake Engineering*, 1-25.
- [5] Surtierra (2011). *Recuperación de la Iglesia San Juda Tadeo de Malloa. Informe Final*. Santiago: Oficina de Arquitectura Surtierra – in Spanish.
- [6] Correia, M., Dipasquale, L., & Mecca, S. (2014). *VERSUS: Heritage for Tomorrow*. Firenze University Press
- [7] Ortega, J., Vasconcelos, G., Rodrigues, H., Correia, M., Lourenço, P.B. (2017). Traditional earthquake resistant techniques for vernacular architecture and local seismic cultures: a literature review. *Journal of Cultural Heritage* 27, 181-196
- [8] Borri, A., Corradi, M., Castori, G., & De Maria, A. (2015). A method for the analysis and classification of historic masonry. *Bulletin of Earthquake Engineering*, 13(9), 2647-2665.
- [9] Instituto Nacional de Normalización (INN), 2013. *Estructuras –Intervención de construcciones patrimoniales de tierra cruda– Requisitos del Proyecto Estructural*. Santiago, Chile NCh3332.Of2013.
- [10] R&V Ingeniero, (2012). *Informe de mecánica de suelos. Iglesia San Judas Tadeo. VI región del Libertador Bernardo O’Higgins*
- [11] Ministerio de Vivienda y Urbanismo – MINVU (Chile). 2011. *Reglamento que fija el diseño sísmico de edificios y deroga D.S. N°117 MINVU of 2010*.
- [12] Instituto Nacional de Normalización (INN), 1996. *Earthquake resistant design of buildings, Official Chilean Code NCh433.Of96*.
- [13] D. M. LL. PP., (2008), *Norme Tecniche per le Costruzioni*, 14 Gennaio, Roma (in Italian).
- [14] G.U. no.55, 7/03/2006. *Approval of forms for the seismic damage assessment of cultural heritage buildings, Decree of the Prime Minister, Rome 23/02/2006*. (in Italian).^
- [15] Eurocode 8, (2004). *Design of structures for earthquake resistance – Part 1: General rules, seismic actions, and rules for buildings (EN 1998-1)*, European Committee of Standardization. Brussels, Belgium; 2004.
- [16] Tarque, N. (2011). *Numerical modelling of the seismic behaviour of adobe buildings*. de Ph. D., University of Pavia.
- [17] Misseri, G., Palazzi, N.C., Rovero, L.(2020) *Seismic vulnerability of timber-reinforced earthen structures through standard and non–standard limit analysis*. *Engineering Structures*.
- [18] Barbisan, U., & Laner, F. (2000). *Capriate e tetti in legno: progetto e recupero: tipologie, esempi di dimensionamento, particolari costruttivi, criteri e tecnologie per il recupero, manti di copertura (Vol. 3)*. FrancoAngeli.
- [19] Casapulla, C., Cascini, L., Portioli, F., & Landolfo, R. (2014). 3D macro and micro-block models for limit analysis of out-of-plane loaded masonry walls with non-associative Coulomb friction. *Meccanica*, 49(7), 1653-1678.
- [20] Casapulla, C., & Argiento, L. U. (2018). In-plane frictional resistances in dry block masonry walls and rocking-sliding failure modes revisited and experimentally validated. *Composites Part B: Engineering*, 132, 197-213.